AFRL-DE-PS-TP-2007-1007

CLOSED-LOOP CONTROL TECHNIQUES FOR AN ADAPTIVE-OPTICAL SYSTEM WITH AN INTERFEROMETRIC WAVEFRONT SENSOR (Postprint)

Laura M. Klein
Troy A. Rhoadarmer

1 September 2006

Conference Proceedings

AIR FORCE RESEARCH LABORATORY
Directed Energy Directorate
3550 Aberdeen Ave SE
AIR FORCE MATERIEL COMMAND
KIRTLAND AIR FORCE BASE, NM 87117-5776

REPORT DOCUMENTATION PAGE

Form Approved
OMB No. 0704-0188

1. REPORT DATE *(DD-MM-YYYY)*	2. REPORT TYPE	3.DATES CIVERED (From-To)
01-09-2006	Conference Proceedings	1 Apr 04 to 1 Sep 06

4. TITLE AND SUBTITLE
Closed-loop Control Techniques for an Adaptive-optical System With an Interferometric Wavefront Sensor (Postprint)

5a. CONTRACT NUMBER
In-House 299962

5b. GRANT NUMBER

5c. PROGRAM ELEMENT NUMBER
063605F

6. AUTHOR(S)
Laura M. Klein, Troy A. Rhoadarmer

5d. PROJECT NUMBER
JT00

5e. TASK NUMBER
S0

5f. WORK UNIT NUMBER
AB

7. PERFORMING ORGANIZATION NAME(S) AND ADDRESS(ES)

AFRL/DES
3550 Aberdeen Ave SE
Kirtland AFB, NM 87117-5776

8. PERFORMING ORGANIZATION REPORT NUMBER

9. SPONSORING / MONITORING AGENCY NAME(S) AND ADDRESS(ES)
AIR FORCE RESEARCH LABORATORY
3550 Aberdeen Ave SE
Kirtland AFB, NM 87117-5776

10. SPONSOR/MONITOR'S ACRONYM(S)
AFRL/DES

11. SPONSOR/MONITOR'S REPORT NUMBER(S)
AFRL-DE-PS-TP-2007-1007

12. DISTRIBUTION / AVAILABILITY STATEMENT

Approved for Public Release; Distribution is Unlimited.

13. SUPPLEMENTARY NOTES
Published in conference proceedings of SPIE Vol. 6306 (2006). GOVERNMENT PURPOSE RIGHTS

14. ABSTRACT
The self-referencing interferometer (SRI) wavefront sensor (WFS) is being developed for applications requiring laser propagation in strong scintillation. Because it directly measures the optical field of the wavefront, the SRI WFS is less effected by scintillation than conventional WFSs. This feature also means the phrase determined from the WFS measurements is limited to the range-pie to pie, due to the use of the arctangent function. If a segmented wavefront corrector is used, this constraint is not a problem. However, if a continuous facesheet deformable mirror is used, the resulting phase should be unwrapped in order to minimize fitting error. There are a couple of places in the adaptive-optical (AO) closed-loop control process where unwrapping algorithm can be inserted. Simulations of these configurations have shown that how and where the unwrapping options and the associated issues. A laboratory demonstration of two control loop configurations was carried out to test the validity of the simulation results. These experiments and their outcome are discussed.

15. SUBJECT TERMS
Adaptive optics, wavefront sensors, interferometers, scintillation, wavefront reconstruction

16. SECURITY CLASSIFICATION OF:			17. LIMITATION OF ABSTRACT	18. NUMBER OF PAGES	19a. NAME OF RESPONSIBLE PERSON
a. REPORT	b. ABSTRACT	c. THIS PAGE			Laura M. Klein
Unclassified	Unclassified	Unclassified	SAR	11	19b. TELEPHONE NUMBER *(include area code)*

Closed-loop control techniques for an adaptive-optical system with an interferometric wavefront sensor

Laura M. Klein and Troy A. Rhoadarmer
Optics Division, AFRL/DES, Directed Energy Directorate,
U.S. Air Force Research Laboratory, Kirtland AFB, NM 87117-5776 USA

ABSTRACT

The self-referencing interferometer (SRI) wavefront sensor (WFS) is being developed for applications requiring laser propagation in strong scintillation. Because it directly measures the optical field of the wavefront, the SRI WFS is less effected by scintillation than conventional WFSs. This feature also means the phase determined from the WFS measurements is limited to the range $-\pi$ to π, due to the use of the arctangent function. If a segmented wavefront corrector is used, this constraint is not a problem. However, if a continuous facesheet deformable mirror is used, the resulting phase should be unwrapped in order to minimize fitting error. There are a couple of places in the adaptive-optical (AO) closed-loop control process where an unwrapping algorithm can be inserted. Simulations of these configurations have shown that how and where the unwrapping is carried out affects overall AO performance and loop stability. This paper presents an overview of the unwrapping options and the associated issues. A laboratory demonstration of two control loop configurations was carried out to test the validity of the simulation results. These experiments and their outcome are discussed.

Keywords: adaptive optics, wavefront sensors, interferometers, scintillation, wavefront reconstruction

1. Introduction

Because the SRI directly measures the optical field, it is capable of detecting branch points in the unwrapped phase and correcting them. In strong scintillation environments, it is essential to improved closed loop performance that branch points are compensated for. Simulations of control algorithms have shown that SRI performance depends on how and where the phase unwrapping and branch point detection occurs. Specifically, unwrapping can occur either before or after the temporal filtering of the reconstructed phase. The values of the filter coefficients have also been shown to affect system performance. This paper documents an experiment conducted to alter the parameters described above and evaluate their effects on system performance. The experiment was conducted in the Atmospheric Simulation and Adaptive optics Laboratory Testbed (ASALT), located at the Starfire Optical Range (SOR), Air Force Research Laboratory, Kirtland Air Force Base, New Mexico.

An overview of the SRI WFS simulation results is given in section 2. Section 3 discusses the unwrapping and filtering procedures for two closed loop control algorithms to be implemented with an SRI WFS. Simulation of the SRI with the two control loops is presented and discussed in section 4. To validate the simulation and analysis, a laboratory investigation of both control methods was conducted, and will be presented in section 5. The results of this effort are detailed in section 6, with closing comments in section 7.

2. Overview of the SRI WFS

The SRI is a phase shifting, point diffraction interferometer[3]. A schematic of the SRI is shown in figure 1. It operates by splitting the incoming beam, U_0, into two beams-the signal, U_S, and reference, U_r, beams. The reference beam is then coupled into a single mode fiber to produce a known reference wavefront, and temporally phase shifted[4]. The resulting reference beam is recombined with the signal beam to produce interference fringes on the WFS camera. From

the resulting interference patterns, the optical field of the beam can be reconstructed. Currently, the SRI employs a fiber phase shifter to temporally phase shift the reference.

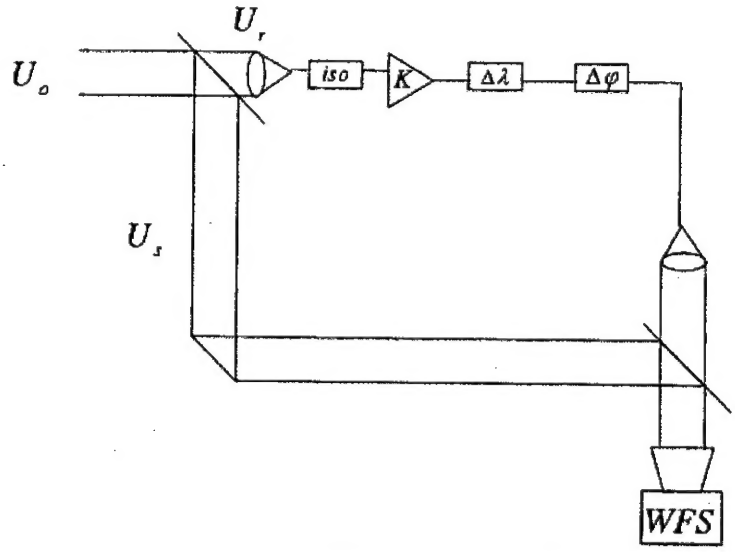

Figure 1. Schematic of the SRI WFS.

3. Filtering and Unwrapping

3.1 Least Squares Unwrapping

When using a continuous facesheet DM, the phase retrieved from the WFS is unwrapped via the arctangent function to exist within the bounds of $-\pi$ and π. The slopes of the incoming phase are extracted by multiplying the phase by the geometry matrix, G, shown in equation 1.

$$\vec{s} = G\vec{\varphi} \tag{1}$$

To determine the least squares phase, the pseudo-inverse of the geometry matrix is applied to the slopes from equation 1. This is mathematically shown in equation 2.

$$\vec{\varphi}_{LS} = (G^T G)^{-1} G^T \vec{s} \tag{2}$$

Replacing $\vec{s}$ in equation 2 with its definition from equation 1 the error is now seen to be

$$\vec{\varepsilon} = (G^T G)^{-1} G^T G\vec{\varphi} \tag{3}$$

Theoretically, the inverse of the geometry matrix multiplied by the geometry matrix should simplify to the identity matrix. However, G is not invertible, and so least squares reconstruction matrix, E, is introduced:

$$E = (G^T G)^{-1} G^T \tag{4}$$

The least squares error in the phase is now obtained from the incoming phase as follows:

$$\vec{\varphi}_{LS} = E\vec{s} \tag{5}$$

3.2 Branch Point Contribution

The process of including branch points to the reconstructed phase is diagrammed in figure 2. The original wrapped phase is subtracted form the reconstructed phase, to extract the branch point phase. The branch point phase is then subtracted from the reconstructed phase, to produce to the total phase.

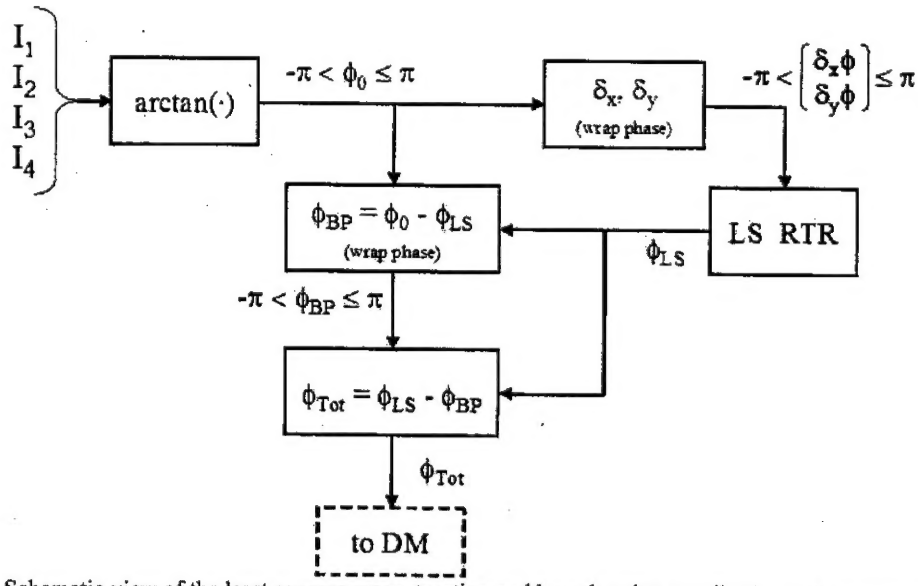

Figure 2. Schematic view of the least squares reconstruction and branch point contribution to the unwrapped phase.

3.3 Temporal Filtering

Before the unwrapped phase is sent as a command to correctly update the DM, it is filtered. The equation for linear temporal filtering is shown in equation 6.

The incoming phase, represented as ε and the previous DM commands, $c(t-1)$, are added together to produce $c(t)$, the commands sent to update the DM. The coefficients for each term in equation 6 are scaling factors that can change the level of influence each term has on producing the updated commands. The coefficient 'a' controls the percentage of the previous commands to be used in updating the current commands. The coefficient 'b' controls the influence of the incoming phase to update the current commands.

$$c(t) = ac(t-1) + b\varepsilon(t-1) \tag{6}$$

3.4 Exponential filtering

With exponential control, the incoming phase is filtered prior to being unwrapped and reconstructed. Since it is the argument of the exponential that determines the phase, the modulo 2π unwrapping is inherently included in the filtering process, therefore, with exponential control, the order in which the phase is filtered matters. After the phase is filtered, the resulting commands are unwrapped and reconstructed in the same manner as the linear unwrapping process described above.

$$\varphi_{\mathrm{mod}2\pi} = \arg\{e^{i[c(t)=ac(t-1)+b\varepsilon(t-1)]}\} \tag{7}$$

4. Simulation of Control Architectures

Because the data from the SRI WFS is fundamentally different than that of a Shack-Hartmann sensor, the control algorithms used to handle the data are also different[1,2]. Before testing prototype control architectures in a laboratory environment, simulation of their affect on an SRI AO system was conducted to evaluate each method. The results of this simulation are presented in figure 3 and shown in red. The resolution of both systems is 1 WFS subaperture to 1 DM actuator (1:1). With the linear control, the loop closes but is unstable, and continually drives the performance down. The exponential control is stable, but highly variant in frame to frame strehl values.

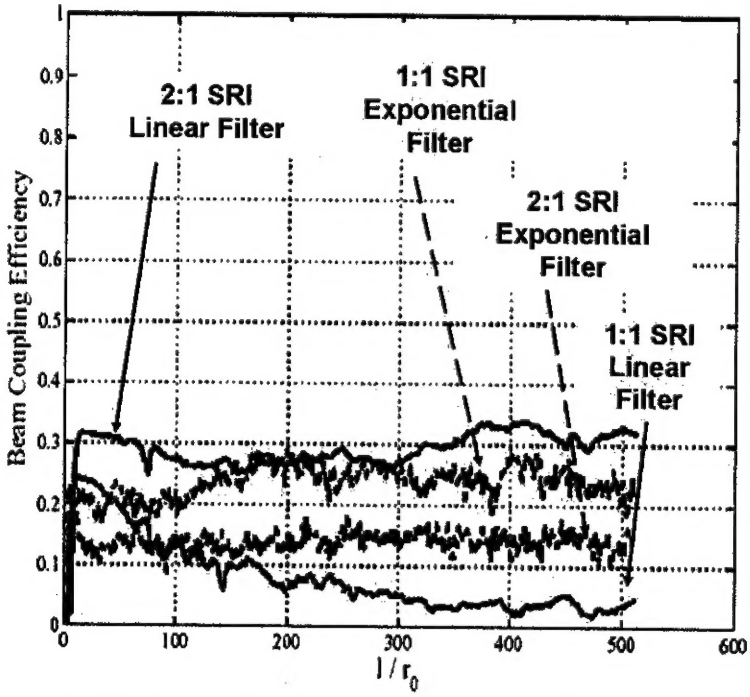

Figure 3. Simulation of an SRI with varying control techniques. The 1:1 resolution for both the linear and exponential control is unstable, however at 2:1 resolution, linear control is stable.

The degradation in performance seen in the linear control case is the result of the low WFS resolution. The SRI can sense the presence of a branch cut, send the appropriate correction to the DM, however, due to the low resolution, cannot see the correction it has just applied, and re-sends the correction for the branch cut, thereby causing an unstable feedback loop. As a result, the DM binds in these areas with supposed branch points.

The variability in the performance with exponential control is an inherent feature of the ordering of unwrapping and filtering within the control process. The phase is filtered before it is unwrapped, causing the information sent to the unwrapper to change from frame to frame. Consequently, the branch cuts "jump" locations from frame to frame, stressing different actuators on the DM at each frame update.

Neither method of control from this simulation offers an acceptable solution to closed-loop control. To alleviate the instability seen from the low resolution, both methods were simulated with the WFS subaperture to DM actuator ratio increased to 2:1. Results of the higher resolution are presented in figure 3 in blue.

With 2:1 linear control, the loop is stable and produces high strehls, indicating the poor performance of linear control at 1:1 resolution was due to not adequately sampling the wavefront. With 2:1 exponential control, the stable mean strehl but high frame to frame variability is identical to the 1:1 exponential control, but the overall performance is degraded.

5. Control Algorithm Experiment

Simulation, as discussed in the previous section, indicates the order of unwrapping and filtering in closed-loop control matters. To effectively verify this in a laboratory environment, an optimal value for the filter coefficients was identified, and with these optimal settings, varied the form of control algorithm.

The experiment examined an AO system utilizing an SRI. To fully characterize the effects of both the filter coefficients and method of control, three turbulence settings were tested. Their values are shown in table1.

Table 1. Turbulence values for the control algorithm experiment. d/r_0 is the number of r_0's per subaperture.

	d/r_0	Rytov
Mild	0.5	0.3
Moderate	0.7	0.5
Strong	0.8	1.0

6. Results

6.1 Filter Coefficients

The 'a' coefficient influences the previous DM commands, and is often referred to as the "leak" factor, as its value determines how the old commands are leaked off the DM. The 'b' coefficient influences the phase error, and is often referred to as the gain.

Table 2. Filter coefficient values and system strehl in weak turbulence for the control algorithm experiment. From this data, an approximate "optimal" value for 'a'= 0.995 and 'b'= 0.16.

'a'	'b'	Strehl
0.995	0.08	0.45
	0.16	0.52
0.97	0.08	0.42
	0.16	0.55
	0.24	0.56
0.95	0.08	0.39
	0.24	0.55

The values of the filter coefficients and the associated closed-loop strehl in weak turbulence are shown in table 2. Ideally, the range covered in testing the 'b' coefficient should span from 0.2 to 0.6, but errors in DM calibrations

adjusted the effective range that was eventually tested. Regardless, the trends indicated in table 2 point toward an acceptable value for 'b' at 0.16. Similarly, 0.995 was an acceptable value for 'a'.

The trends seen for the coefficients in strong turbulence match those described above and the specific values are seen in table 3.

Table 3. Filter coefficient values and system strehl in strong turbulence for the control algorithm experiment. This data confirms the selected "optimal" values 'a'= 0.995 and 'b'= 0.16.

'a'	'b'	Strehl
0.995	0.08	0.33
	0.16	0.39
0.95	0.08	0.29
	0.24	0.43

6.2 Control Method

Figure 4 shows the characteristics of both control algorithms for both the 1:1 and 2:1 resolutions of the WFS in weak turbulence.

The blue line shows the performance of the 1:1 linear control. The time history shows the loops initially closes, but begins to taper down. While not as prominent as the 1:1 linear simulation performance, the underlying effect is there, and would be seen if the data run could extended several hundred frames more.

Performance of 2:1 linear control is shown in black. As simulation predicts, linear control at this resolution is stable during closed loop and produces high strehls.

1:1 exponential control is shown in red. It is stable in closed loop, produces high strehls, and performs comparably to 2:1 linear. While somewhat variant in frame to frame strehl, it does not exhibit the exaggerated characteristics predicted by simulation.

2:1 exponential control is displayed in green. Like simulation, strehl values vary greatly from frame to frame, but has an overall mean strehl that is high. Its performance is lower than that of the 1:1 exponential, also as predicted by simulation.

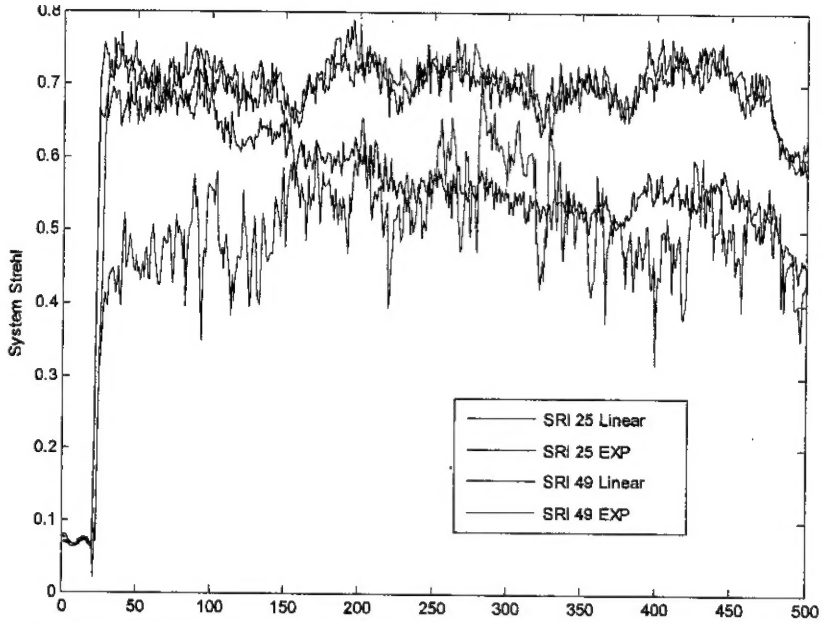

Figure 4. SRI system performance of exponential and linear control in weak turbulence, with filter coefficient 'a' = 0.995 and 'b' = 0.16. 1:1 linear is shown in blue, 2:1 linear in black, 1:1 exponential in red, and 2:1 exponential in green.

Figure 5 shows the characteristics of both control algorithms for both the 1:1 and 2:1 resolutions of the WFS in strong turbulence.

Again, 1:1 linear control is delineated in blue. Its performance traits are strongly in agreement with simulation predictions. The dramatic performance degradation clearly mimics the pattern seen in simulation.

2:1 linear control is shown in black and exhibits the same stable performance seen in simulation.

1:1 exponential control is presented by the red line, and performs comparably to the 2:1 linear control. With the stronger turbulence, this method of control seems to have slightly more variance than that of the linear control, but far less than the simulation predictions.

2:1 exponential control is in green, and like simulation and the weaker turbulence case, has reduced performance in comparison to the 1:1 exponential, with highly varying strehl values from frame to frame.

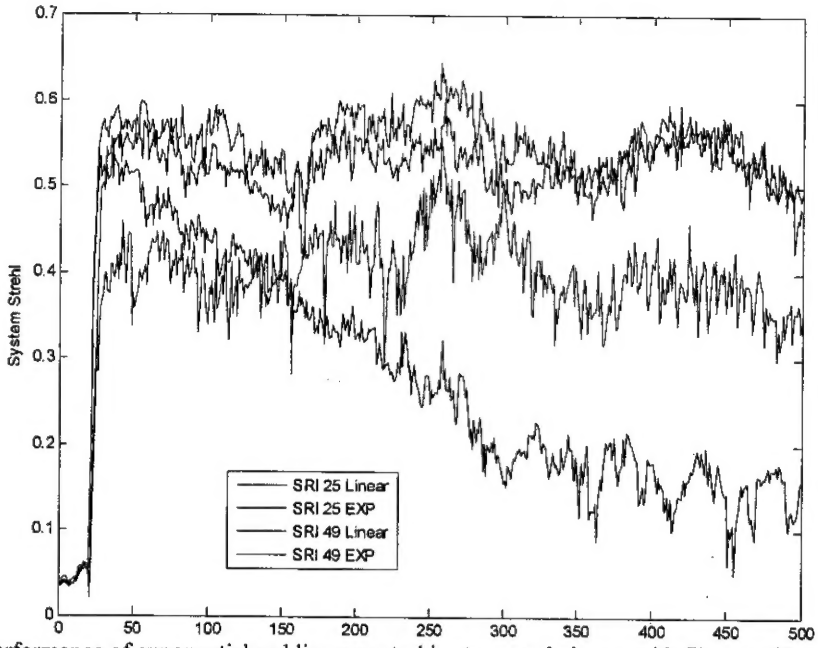

Figure 5. SRI system performance of exponential and linear control in strong turbulence, with filter coefficient 'a' = 0.995 and 'b' = 0.16. 1:1 linear is shown in blue, 2:1 linear in black, 1:1 exponential in red, and 2:1 exponential in green.

7. Summary

This paper describes simulation and a laboratory experiment conducted to investigate the characteristics of two different control methods and filter coefficients.

Simulation shows that at lower resolutions (1 subaperture to 1 DM actuator), linear control is unstable, but high resolution (2 subapertures to 1 DM actuator) sufficiently overcomes the stability issue. Exponential control is stable but highly variant for both resolutions, with a degradation in performance at the higher resolution.

From the trends seen in system performance while varying the filter coefficients, the value of 0.995 was identified as an appropriate value for the 'a' coefficient, and 0.16 for the 'b' coefficient. Using these "good" values for the filter coefficients, exponential and linear control algorithms were tested on an SRI AO system, with varying turbulence and varying resolution values. The results were compared against simulation.

1:1 linear control was unstable in closed loop, due to poor resolution. 2:1 linear control was stable and produced high strehls. 1:1 exponential control was somewhat variant in frame to frame strehl, but had a high mean closed-loop strehl. 2:1 exponential control was highly variant in frame to frame strehl, and had lower performance in comparison to the 1:1 exponential control.

Laboratory results match well with simulation, which validates modeling and theory. The cause behind the degraded performance seen with the 2:1 exponential control has yet to be explained, and will be further investigated in the future.

References

1. J. D. Barchers, D.L. Fried, and D.J. Link, "Evaluation of the performance of Hartmann sensors in strong scintillation," *Appl. Opt.* **41**, pp 1012-1021, 2002.
2. J. D. Barchers, D.L. Fried, and D.J. Link, G. A. Tyler, W. Moretti, T. J. Brennan, and R. Q. Fugate, "Performance of wavefront sensors in strong scintillation," in *Adaptive Optical Systems Technologies II*, P. L. Wizinowich and D. Bonaccini, eds., *Proc. SPIE* **4839**, pp 217-227, 2003.

3. T. A. Rhoadarmer, "Development of the self-referencing interferometer wavefront sensor", in *Advanced Wavefront Control: Methods, Devices, and Applications II*, J. D. Gonglewski and M. T. Gruneisen and M. K. Giles, eds., *Proc. SPIE* **5553**, 2004.
4. M. S. Corley, and T. A. Rhoadarmer, "Evaluation of phase shifting techniques for a self referencing interferometer wavefront sensor in strong scintillation" in *Advanced Wavefront Control: Methods, Devices, and Applications III*, J. D. Gonglewski and M. T. Gruneisen and M. K. Giles, eds., *Proc.SPIE* **5894**, 2005.
5. S. J. Mantravadi, T. A. Rhoadarmer, and R. S. Glas, "A simple laboratorysystem for generating well-controlled atmospheric-like turbulence," in *Advanced Wavefront Control: Methods, Devices, and Applications III*, J. D. Gonglewski and M. T. Gruneisen and M. K. Giles, eds., *Proc.SPIE* **5553**, pp. 290-300, 2004.